

# Synthesis of lithium $\text{LiNi}_{1-y}\text{Co}_y\text{O}_2$ from lithium carbonate, nickel oxide and cobalt carbonate and their electrochemical properties

Ho Rim <sup>a</sup>, Hye Ryoung Park <sup>b</sup>, Myoung Youp Song <sup>c,\*</sup>

<sup>a</sup> ASE Korea, 494 Munbal-dong Paju-si Gyeonggi-do, 413-790, Republic of Korea

<sup>b</sup> School of Applied Chemical Engineering, Chonnam National University, 300 Yongbong-dong Buk-gu Gwangju, 500-757, Republic of Korea

<sup>c</sup> Division of Advanced Materials Engineering, Hydrogen & Fuel Cell Research Center, Engineering Research Institute, Chonbuk National University, 567 Baekje-daero Deokjin-gu Jeonju, 561-756, Republic of Korea

Received 13 April 2012; accepted 17 April 2012

Available online 24 April 2012

## Abstract

$\text{LiNi}_{1-y}\text{Co}_y\text{O}_2$  ( $y = 0.1, 0.3$  and  $0.5$ ) were synthesized by solid state reaction method at  $800^\circ\text{C}$  and  $850^\circ\text{C}$  from  $\text{Li}_2\text{CO}_3$ ,  $\text{NiO}$  and  $\text{CoCO}_3$  as starting materials. The electrochemical properties of the synthesized  $\text{LiNi}_{1-y}\text{Co}_y\text{O}_2$  were investigated. As the content of Co decreases, particle size decreases rapidly and particle size gets more homogeneous. When the particle size is compared at the same composition, the particles synthesized at  $850^\circ\text{C}$  are larger than those synthesized at  $800^\circ\text{C}$ . Among  $\text{LiNi}_{1-y}\text{Co}_y\text{O}_2$  ( $y = 0.1, 0.3$  and  $0.5$ ) synthesized at  $850^\circ\text{C}$ ,  $\text{LiNi}_{0.7}\text{Co}_{0.3}\text{O}_2$  has the largest intercalated and deintercalated Li quantity  $\Delta x$  at the first charge–discharge cycle, followed in order by  $\text{LiNi}_{0.9}\text{Co}_{0.1}\text{O}_2$  and  $\text{LiNi}_{0.5}\text{Co}_{0.5}\text{O}_2$ .  $\text{LiNi}_{0.7}\text{Co}_{0.3}\text{O}_2$  synthesized at  $850^\circ\text{C}$  has the largest first discharge capacity (142 mAh/g), followed in order by  $\text{LiNi}_{0.9}\text{Co}_{0.1}\text{O}_2$  synthesized at  $850^\circ\text{C}$  (113 mAh/g), and  $\text{LiNi}_{0.5}\text{Co}_{0.5}\text{O}_2$  synthesized at  $800^\circ\text{C}$  (109 mAh/g).

© 2012 Elsevier Ltd and Techna Group S.r.l. All rights reserved.

**Keywords:**  $\text{LiNi}_{1-y}\text{Co}_y\text{O}_2$ ; Solid state reaction method; Voltage vs.  $x$  in  $\text{Li}_x\text{Ni}_{1-y}\text{Co}_y\text{O}_2$  curve; Discharge capacity

## 1. Introduction

$\text{LiCoO}_2$  [1–4],  $\text{LiNiO}_2$  [5–13], and  $\text{LiMn}_2\text{O}_4$  [14–20] have been studied by many researchers as cathode materials for lithium secondary batteries [21].  $\text{LiMn}_2\text{O}_4$  is relatively inexpensive and environment-friendly, but its cycling performance is poor.  $\text{LiCoO}_2$  has a large diffusivity and a high operating voltage, and its preparation is easy. However, it has a disadvantage that it contains an expensive element, Co.

$\text{LiNiO}_2$  is a very promising cathode material since it has a large discharge capacity [22] and is relatively excellent from the viewpoints of economics and environment. However, due to the similarity of Li and Ni ionic sizes ( $\text{Li}^+ = 0.72 \text{ \AA}$  and  $\text{Ni}^{2+} = 0.69 \text{ \AA}$ ), the  $\text{LiNiO}_2$  is practically obtained in the non-stoichiometric compositions,  $\text{Li}_{1-y}\text{Ni}_{1+y}\text{O}_2$  [23,24], and the  $\text{Ni}^{2+}$  ions in lithium planes obstruct the movement of the  $\text{Li}^+$  ions during charge and discharge [25,26].

The shortcomings of  $\text{LiCoO}_2$  and  $\text{LiNiO}_2$  can be overcome by incorporating these phases into  $\text{LiNi}_{1-y}\text{Co}_y\text{O}_2$  compositions because the presence of cobalt stabilizes the structure in a strictly two-dimensional fashion, thus favoring good reversibility of the intercalation and deintercalation reactions [25,27–35]. Rougier et al. [25] reported that the stabilization of the two-dimensional character of the structure by cobalt substitution in  $\text{LiNiO}_2$  is correlated with an increase in the cell performance, due to the decrease in the amount of extra-nickel ions in the inter-slab space which impede the lithium diffusion. Kang et al. [35] investigated the structure and electrochemical properties of the  $\text{Li}_x\text{Co}_y\text{Ni}_{1-y}\text{O}_2$  ( $y = 0.1, 0.3, 0.5, 0.7$  and  $1.0$ ) system synthesized by solid state reaction with various starting materials to optimize the characteristics and synthetic conditions of the  $\text{Li}_x\text{Co}_y\text{Ni}_{1-y}\text{O}_2$ . The first discharge capacities of  $\text{Li}_x\text{Co}_y\text{Ni}_{1-y}\text{O}_2$  were 60–180 mAh/g depending on synthetic conditions.

In this work,  $\text{LiNi}_{1-y}\text{Co}_y\text{O}_2$  ( $y = 0.1, 0.3$  and  $0.5$ ) cathode materials were synthesized by solid state reaction method at different temperatures using  $\text{Li}_2\text{CO}_3$ ,  $\text{NiO}$  and  $\text{CoCO}_3$  as starting materials. The electrochemical properties of the synthesized samples were then investigated.

\* Corresponding author. Tel.: +82 63 270 2379; fax: +82 63 270 2386.

E-mail address: [songmy@jbnu.ac.kr](mailto:songmy@jbnu.ac.kr) (M.Y. Song).

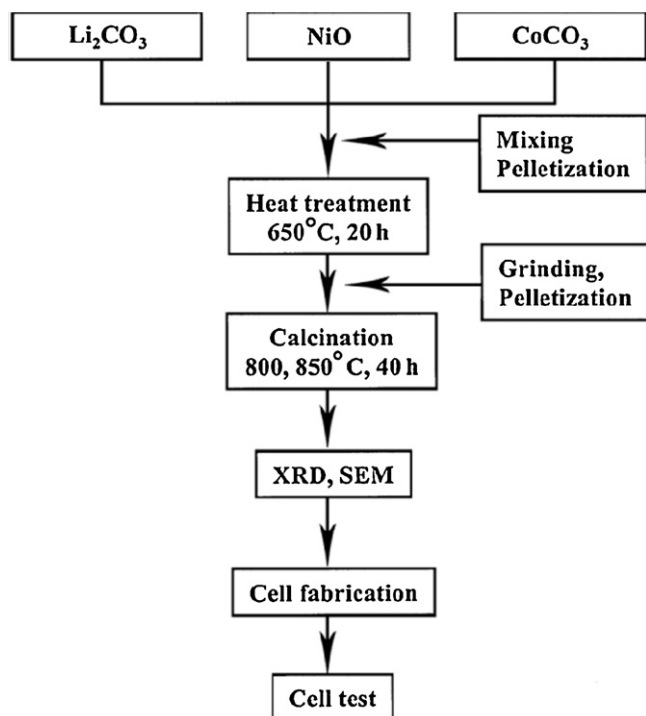


Fig. 1. Experimental procedure for  $\text{LiNi}_{1-y}\text{Co}_y\text{O}_2$  synthesis from  $\text{Li}_2\text{CO}_3$ ,  $\text{NiO}$  and  $\text{CoCO}_3$  and characterization.

## 2. Experimental

$\text{Li}_2\text{CO}_3$ ,  $\text{NiO}$  and  $\text{CoCO}_3$  were used as starting materials to synthesize  $\text{LiNi}_{1-y}\text{Co}_y\text{O}_2$  by the solid-state reaction method. All the starting materials (with the purity 99.9%) were purchased from Aldrich Co.

The experimental procedure for  $\text{LiNi}_{1-y}\text{Co}_y\text{O}_2$  synthesis from  $\text{Li}_2\text{CO}_3$ ,  $\text{NiO}$  and  $\text{CoCO}_3$  and characterization is given schematically in Fig. 1. The mixture of starting materials in the compositions of  $\text{LiNi}_{1-y}\text{Co}_y\text{O}_2$  ( $y = 0.1, 0.3$  and  $0.5$ ) was mixed sufficiently and pelletized. This pellet was heat treated in air at  $650^\circ\text{C}$  for 20 h. It was then ground, mixed, pelletized and calcined at  $800^\circ\text{C}$  or  $850^\circ\text{C}$  for 20 h. This pellet was cooled at

a cooling rate of  $50^\circ\text{C}/\text{min}$ , ground, mixed and again pelletized. It was then calcined again at  $800^\circ\text{C}$  or  $850^\circ\text{C}$  for 20 h.

The phase identification of the synthesized samples was carried out by X-ray diffraction (XRD) analysis using  $\text{Cu K}\alpha$  radiation (Mac-Science Co., Ltd.). The scanning rate was  $16^\circ/\text{min}$  and the scanning range of diffraction angle ( $2\theta$ ) is  $10^\circ \leq 2\theta \leq 70^\circ$ . The morphologies of the samples were observed using a scanning electron microscope (SEM).

The electrochemical cells consisted of  $\text{LiNi}_{1-y}\text{Co}_y\text{O}_2$  as a positive electrode, Li foil as a negative electrode, and electrolyte of 1 M  $\text{LiPF}_6$  in a 1:1 (volume ratio) mixture of ethylene carbonate (EC) and dimethyl carbonate (DMC). A Whatman glass-fiber was used as the separator. The cells were assembled in an argon-filled dry box. To fabricate the positive electrode, 89 wt% synthesized oxide, 10 wt% acetylene black, and 1 wt% polytetrafluoroethylene (PTFE) binder were mixed in an agate mortar. By introducing Li metal, Whatman glass-fiber, positive electrode, and the electrolyte, the cell was assembled. All the electrochemical tests were performed at room temperature with a potentiostatic/galvanostatic system (Mac-Pile system, Bio-Logic Co. Ltd.). The cells were cycled at a current density of  $200 \mu\text{A}/\text{cm}^2$  in a voltage range of 3.2–4.3 V.

## 3. Results and discussion

XRD patterns of  $\text{LiNi}_{1-y}\text{Co}_y\text{O}_2$  ( $y = 0.1, 0.3$  and  $0.5$ ) powders calcined at  $800^\circ\text{C}$  or  $850^\circ\text{C}$  for 40 h using  $\text{LiOH}\cdot\text{H}_2\text{O}$ ,  $\text{NiO}$  and  $\text{Co}_3\text{O}_4$  as starting materials were identified as corresponding to a  $\alpha\text{-NaFeO}_2$  structure with a space group of  $R\bar{3}m$ .

SEM micrographs of  $\text{LiNi}_{1-y}\text{Co}_y\text{O}_2$  ( $y = 0.1, 0.3$  and  $0.5$ ) synthesized from  $\text{Li}_2\text{CO}_3$ ,  $\text{NiO}$  and  $\text{CoCO}_3$  at  $800^\circ\text{C}$  showed that the particle sizes were not homogeneous and  $\text{LiNi}_{0.5}\text{Co}_{0.5}\text{O}_2$  had the largest particles. As the content of Co decreased, particle size decreased from  $y = 0.5$  to  $y = 0.3$  and increased from  $y = 0.3$  to  $y = 0.1$ .

Fig. 2 exhibits SEM micrographs of  $\text{LiNi}_{1-y}\text{Co}_y\text{O}_2$  ( $y = 0.1, 0.3$  and  $0.5$ ) synthesized from  $\text{Li}_2\text{CO}_3$ ,  $\text{NiO}$  and  $\text{CoCO}_3$  at

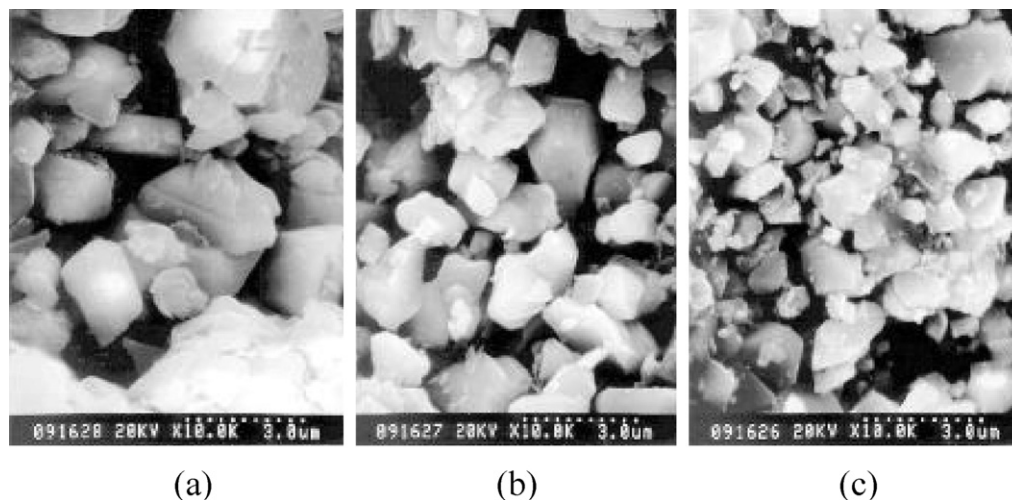


Fig. 2. SEM micrographs of  $\text{LiNi}_{1-y}\text{Co}_y\text{O}_2$  synthesized from  $\text{Li}_2\text{CO}_3$ ,  $\text{NiO}$  and  $\text{CoCO}_3$  at  $850^\circ\text{C}$ ; (a)  $y = 0.5$ , (b)  $y = 0.3$ , and (c)  $y = 0.1$ .

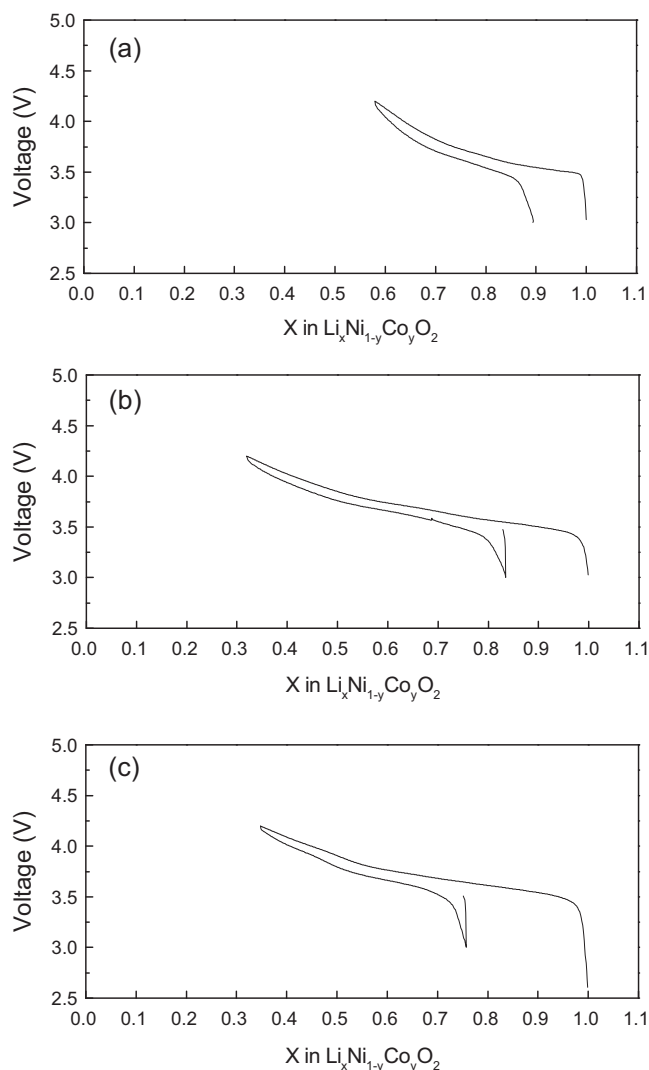


Fig. 3. Voltage vs.  $x$  in  $\text{Li}_x\text{Ni}_{1-y}\text{Co}_y\text{O}_2$  curves for the first charge–discharge at a current density of  $200 \mu\text{A}/\text{cm}^2$  of  $\text{LiNi}_{1-y}\text{Co}_y\text{O}_2$  synthesized at  $850^\circ\text{C}$ ; (a)  $y = 0.5$ , (b)  $y = 0.3$ , and (c)  $y = 0.1$ .

$850^\circ\text{C}$ . The particles have round surfaces. As the content of Co decreases, particle size decreases rapidly and particle size gets more homogeneous. When the particle size is compared at the same composition, the particles synthesized at  $850^\circ\text{C}$  were larger than those synthesized at  $800^\circ\text{C}$ .

Voltage vs.  $x$  in  $\text{Li}_x\text{Ni}_{1-y}\text{Co}_y\text{O}_2$  curves at a current density of  $200 \mu\text{A}/\text{cm}^2$  for the first charge–discharge of  $\text{LiNi}_{1-y}\text{Co}_y\text{O}_2$  synthesized at  $850^\circ\text{C}$  are shown in Fig. 3. The curves exhibit small polarizations, which are the changes in potentials for deintercalation and intercalation of lithium atoms. First charge–discharge curves of  $\text{LiNi}_{0.7}\text{Co}_{0.3}\text{O}_2$  exhibit quite long plateaus. Among  $\text{LiNi}_{1-y}\text{Co}_y\text{O}_2$  ( $y = 0.1, 0.3$  and  $0.5$ ) synthesized at  $850^\circ\text{C}$ ,  $\text{LiNi}_{0.7}\text{Co}_{0.3}\text{O}_2$  has the largest intercalated and deintercalated Li quantity  $\Delta x$ , followed in order by  $\text{LiNi}_{0.9}\text{Co}_{0.1}\text{O}_2$  and  $\text{LiNi}_{0.5}\text{Co}_{0.5}\text{O}_2$ .

Fig. 4 presents voltage vs.  $x$  in  $\text{Li}_x\text{Ni}_{1-y}\text{Co}_y\text{O}_2$  curves for the first and second charge–discharge of  $\text{LiNi}_{0.7}\text{Co}_{0.3}\text{O}_2$  synthesized at  $800^\circ\text{C}$  and  $850^\circ\text{C}$ . The  $\text{LiNi}_{0.7}\text{Co}_{0.3}\text{O}_2$  synthesized at

$850^\circ\text{C}$  shows a larger value of  $\Delta x$  than that of the  $\text{LiNi}_{0.7}\text{Co}_{0.3}\text{O}_2$  synthesized at  $800^\circ\text{C}$ .

First charge capacities at a current density of  $200 \mu\text{A}/\text{cm}^2$  in the voltage range of 3.0–4.3 V for  $\text{LiNi}_{1-y}\text{Co}_y\text{O}_2$  synthesized at  $800^\circ\text{C}$  and at  $850^\circ\text{C}$  are shown in Fig. 5.  $\text{LiNi}_{0.7}\text{Co}_{0.3}\text{O}_2$  synthesized at  $850^\circ\text{C}$  has the largest first discharge capacity, followed in order by  $\text{LiNi}_{0.9}\text{Co}_{0.1}\text{O}_2$  synthesized at  $850^\circ\text{C}$ ,  $\text{LiNi}_{0.5}\text{Co}_{0.5}\text{O}_2$  synthesized at  $800^\circ\text{C}$ ,  $\text{LiNi}_{0.7}\text{Co}_{0.3}\text{O}_2$  synthesized at  $800^\circ\text{C}$ ,  $\text{LiNi}_{0.9}\text{Co}_{0.1}\text{O}_2$  synthesized at  $800^\circ\text{C}$ , and  $\text{LiNi}_{0.5}\text{Co}_{0.5}\text{O}_2$  synthesized at  $850^\circ\text{C}$ .

Fig. 6 presents the variation of the first charge capacity with the value of  $y$  for  $\text{LiNi}_{1-y}\text{Co}_y\text{O}_2$  synthesized at  $800^\circ\text{C}$  and  $850^\circ\text{C}$ .  $\text{LiNi}_{0.7}\text{Co}_{0.3}\text{O}_2$  synthesized at  $850^\circ\text{C}$  has the largest first discharge capacity (142 mAh/g), followed in order by  $\text{LiNi}_{0.9}\text{Co}_{0.1}\text{O}_2$  synthesized at  $850^\circ\text{C}$  (113 mAh/g),  $\text{LiNi}_{0.5}\text{Co}_{0.5}\text{O}_2$  synthesized at  $800^\circ\text{C}$  (109 mAh/g),  $\text{LiNi}_{0.7}\text{Co}_{0.3}\text{O}_2$  synthesized at  $800^\circ\text{C}$  (103 mAh/g),  $\text{LiNi}_{0.9}\text{Co}_{0.1}\text{O}_2$  synthesized at  $800^\circ\text{C}$  (98 mAh/g), and  $\text{LiNi}_{0.5}\text{Co}_{0.5}\text{O}_2$  synthesized at  $850^\circ\text{C}$  (95 mAh/g).

The variations of discharge capacity with number of cycles for  $\text{LiNi}_{1-y}\text{Co}_y\text{O}_2$  ( $y = 0.1, 0.3$  and  $0.5$ ) synthesized at  $800^\circ\text{C}$  and for  $\text{LiNi}_{1-y}\text{Co}_y\text{O}_2$  ( $y = 0.3$  and  $0.5$ ) synthesized at  $850^\circ\text{C}$  are shown in Fig. 7.  $\text{LiNi}_{0.9}\text{Co}_{0.1}\text{O}_2$  synthesized at  $850^\circ\text{C}$  has the largest first discharge capacity (113 mAh/g), followed in order by  $\text{LiNi}_{0.5}\text{Co}_{0.5}\text{O}_2$  synthesized at  $800^\circ\text{C}$  (109 mAh/g),  $\text{LiNi}_{0.7}\text{Co}_{0.3}\text{O}_2$  synthesized at  $800^\circ\text{C}$  (103 mAh/g),  $\text{LiNi}_{0.9}\text{Co}_{0.1}\text{O}_2$  synthesized at  $800^\circ\text{C}$  (98 mAh/g), and  $\text{LiNi}_{0.5}\text{Co}_{0.5}\text{O}_2$

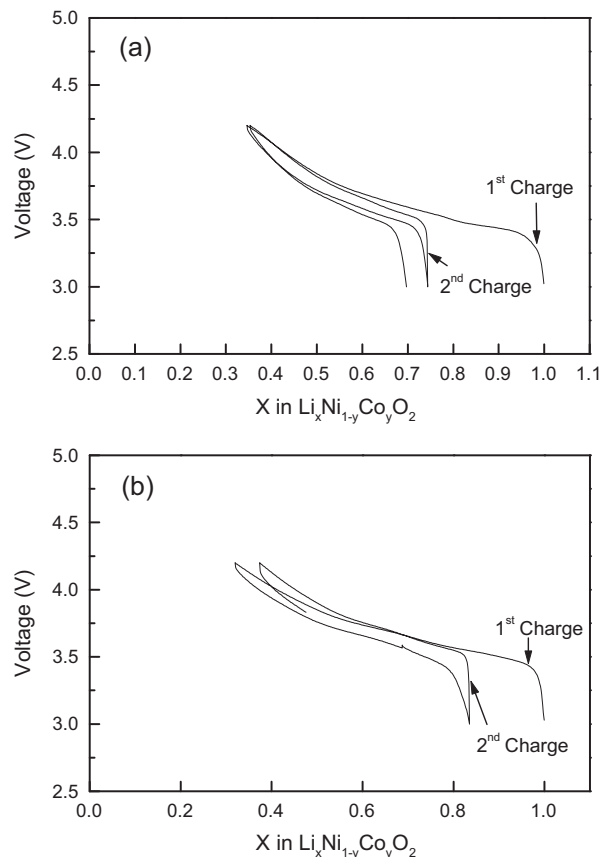


Fig. 4. Voltage vs.  $x$  in  $\text{Li}_x\text{Ni}_{1-y}\text{Co}_y\text{O}_2$  curves for the first and second charge–discharge of  $\text{LiNi}_{0.7}\text{Co}_{0.3}\text{O}_2$  synthesized (a) at  $800^\circ\text{C}$ , and (b) at  $850^\circ\text{C}$ .

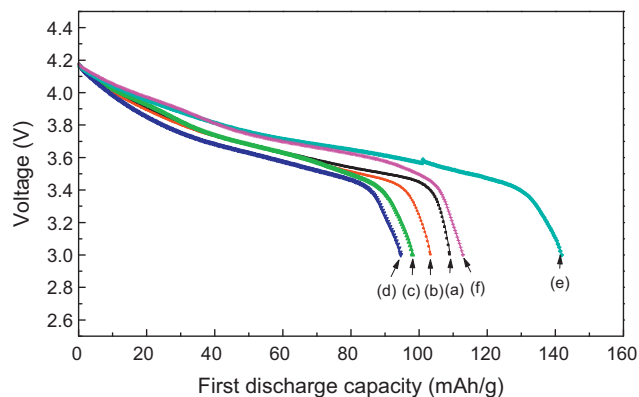


Fig. 5. First discharge capacity at a current density of  $200 \mu\text{A}/\text{cm}^2$  in the voltage range of 3.0–4.3 V for  $\text{LiNi}_{1-y}\text{Co}_y\text{O}_2$  synthesized at  $800^\circ\text{C}$ ; (a)  $y = 0.5$ , (b)  $y = 0.3$ , and (c)  $y = 0.1$ , and at  $850^\circ\text{C}$ ; (d)  $y = 0.5$ , (e)  $y = 0.3$ , and (f)  $y = 0.1$ .

synthesized at  $850^\circ\text{C}$  (95 mAh/g).  $\text{LiNi}_{1-y}\text{Co}_y\text{O}_2$  ( $y = 0.1, 0.3$  and  $0.5$ ) synthesized at  $800^\circ\text{C}$  have very similar cycling behavior.  $\text{LiNi}_{1-y}\text{Co}_y\text{O}_2$  ( $y = 0.1, 0.3$  and  $0.5$ ) synthesized at  $850^\circ\text{C}$  have better cycling performances than those synthesized at  $800^\circ\text{C}$ .  $\text{LiNi}_{0.9}\text{Co}_{0.1}\text{O}_2$  synthesized at  $850^\circ\text{C}$  with the largest discharge capacity has quite good cycling performance with the discharge capacity of 94 mAh/g at the fifth cycle.

The voltage vs.  $x$  in  $\text{Li}_x\text{Ni}_{1-y}\text{Co}_y\text{O}_2$  curves at a current density of  $200 \mu\text{A}/\text{cm}^2$  for the first charge–discharge of  $\text{LiNi}_{1-y}\text{Co}_y\text{O}_2$  synthesized at  $850^\circ\text{C}$  in Fig. 3 show that, as compared with the quantity of the deintercalated Li ions by the first charging, that of the intercalated Li ions by the first discharging is much smaller, which is revealed by the difference in  $\Delta x$  of the first charge and discharge curves, for all the samples. The lengths of plateaus in the charge and discharge curves are proportional to charge and discharge capacities. During the first charging, Li ions deintercalate not only from stable 3b sites but also from unstable 3b sites. After deintercalation from unstable 3b sites, the unstable 3b sites will be destroyed. This is considered to lead to smaller quantity of the intercalated Li ions by the first discharging than that of the deintercalated Li ions by the first charging.

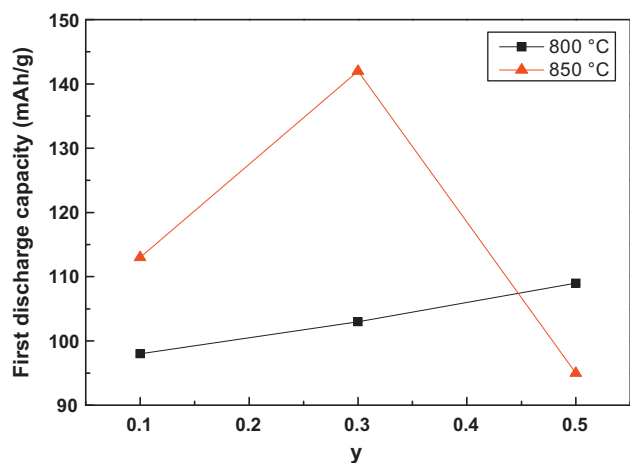


Fig. 6. Variations of the first charge capacity with value of  $y$  for  $\text{LiNi}_{1-y}\text{Co}_y\text{O}_2$  synthesized at  $800^\circ\text{C}$  and  $850^\circ\text{C}$ .

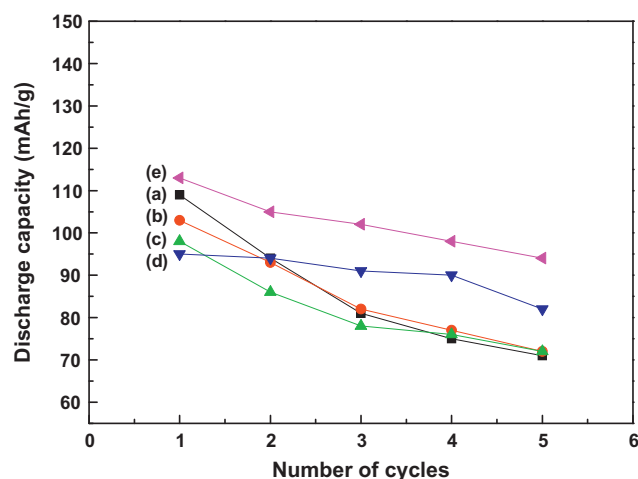


Fig. 7. Variations of discharge capacity with number of cycles for  $\text{LiNi}_{1-y}\text{Co}_y\text{O}_2$  synthesized at  $800^\circ\text{C}$ ; (a)  $y = 0.5$ , (b)  $y = 0.3$ , and (c)  $y = 0.1$ , and at  $850^\circ\text{C}$ ; (d)  $y = 0.5$ , and (e)  $y = 0.1$ .

In the voltage vs.  $x$  in  $\text{Li}_x\text{Ni}_{1-y}\text{Co}_y\text{O}_2$  curves for the first and second charge–discharge of  $\text{LiNi}_{0.7}\text{Co}_{0.3}\text{O}_2$  synthesized at  $800^\circ\text{C}$  and  $850^\circ\text{C}$  in Fig. 4, the charge–discharge curves exhibit quite long plateaus, where two phases co-exist [36]. Arai et al. [37] reported that, during charging and discharging,  $\text{LiNiO}_2$  goes through three phase transitions; phase transitions from hexagonal structure (H1) to monoclinic structure (M), from monoclinic structure (M) to hexagonal structure (H2), and from hexagonal structure (H2) to hexagonal structure (H3) or vice versa. Ohzuku et al. [38] reported that, during charging and discharging,  $\text{LiNiO}_2$  goes through four phase transitions; phase transitions from H1 to M, from M to H2, from H2 to hexagonal structures H2 + H3, and from H2 + H3 to H3 or vice versa. Song et al. [39] reported that  $-dx/dV$  vs.  $V$  curves of  $\text{LiNi}_{1-y}\text{Ti}_y\text{O}_2$  ( $y = 0.012$  and  $0.025$ ) for charging and discharging showed four peaks, revealing the four phase transitions from H1 to M, from M to H2, from H2 to H2 + H3, and from H2 + H3 to H3 or vice versa.

#### 4. Conclusions

$\text{LiNi}_{1-y}\text{Co}_y\text{O}_2$  ( $y = 0.1, 0.3$  and  $0.5$ ) were synthesized from  $\text{Li}_2\text{CO}_3$ ,  $\text{NiO}$  and  $\text{CoCO}_3$  as starting materials by solid state reaction method, in which mixtures with compositions of  $\text{LiNi}_{1-y}\text{Co}_y\text{O}_2$  ( $y = 0.1, 0.3$  and  $0.5$ ) were heat treated in air at  $650^\circ\text{C}$  for 20 h, and then calcined at  $800^\circ\text{C}$  or  $850^\circ\text{C}$  for 40 h. As the content of Co decreases, particle size decreases rapidly and particle size gets more homogeneous. Among  $\text{LiNi}_{1-y}\text{Co}_y\text{O}_2$  ( $y = 0.1, 0.3$  and  $0.5$ ) synthesized at  $850^\circ\text{C}$ ,  $\text{LiNi}_{0.7}\text{Co}_{0.3}\text{O}_2$  has the largest intercalated and deintercalated Li quantity  $\Delta x$  at the first charge–discharge cycle, followed in order by  $\text{LiNi}_{0.9}\text{Co}_{0.1}\text{O}_2$  and  $\text{LiNi}_{0.5}\text{Co}_{0.5}\text{O}_2$ .  $\text{LiNi}_{0.7}\text{Co}_{0.3}\text{O}_2$  synthesized at  $850^\circ\text{C}$  has the largest first discharge capacity (142 mAh/g), followed in order by  $\text{LiNi}_{0.9}\text{Co}_{0.1}\text{O}_2$  synthesized at  $850^\circ\text{C}$  (113 mAh/g), and  $\text{LiNi}_{0.5}\text{Co}_{0.5}\text{O}_2$  synthesized at  $800^\circ\text{C}$  (109 mAh/g).  $\text{LiNi}_{1-y}\text{Co}_y\text{O}_2$  ( $y = 0.1, 0.3$  and  $0.5$ )



synthesized at 850 °C have better cycling performances than those synthesized at 800 °C.

## References

- [1] K. Ozawa, Lithium-ion rechargeable batteries with LiCoO<sub>2</sub> and carbon electrodes: the LiCoO<sub>2</sub>/C system, *Solid State Ionics* 69 (1994) 212–221.
- [2] R. Alcántara, P. Lavela, J.L. Tirado, R. Stoyanova, E. Zhecheva, Structure and electrochemical properties of boron-doped LiCoO<sub>2</sub>, *Journal of Solid State Chemistry* 134 (1997) 265–273.
- [3] Y. Kim, G.M. Veith, J. Nanda, R.R. Unocic, M. Chi, N.J. Dudney, High voltage stability of LiCoO<sub>2</sub> particles with a nano-scale Lipon coating, *Electrochimica Acta* 56 (19) (2011) 6573–6580.
- [4] W.D. Yang, C.Y. Hsieh, H.J. Chuang, Y.S. Chen, Preparation and characterization of nanometric-sized LiCoO<sub>2</sub> cathode materials for lithium batteries by a novel sol-gel method, *Ceramics International* 36 (1) (2010) 135–140.
- [5] J.R. Dahn, U. von Sacken, C.A. Michal, Structure and electrochemistry of Li<sub>1-y</sub>NiO<sub>2</sub> and a new Li<sub>2</sub>NiO<sub>2</sub> phase with the Ni(OH)<sub>2</sub> structure, *Solid State Ionics* 44 (1990) 87–97.
- [6] J.R. Dahn, U. von Sacken, M.W. Juskow, H. Al-Janaby, Rechargeable LiNiO<sub>2</sub>/carboncells, *Journal of the Electrochemical Society* 138 (1991) 2207–2212.
- [7] W. Ebner, D. Fouchard, L. Xie, The LiNiO<sub>2</sub>/carbon lithium-ion battery, *Solid State Ionics* 69 (1994) 238–256.
- [8] H.U. Kim, D.R. Mumm, H.R. Park, M.Y. Song, Synthesis by a simple combustion method and electrochemical properties of LiCo<sub>1/3</sub>Ni<sub>1/3</sub>Mn<sub>1/3</sub>O<sub>2</sub>, *Electronic Materials Letters* 6 (3) (2010) 91–95.
- [9] S.H. Ju, J.H. Kim, Y.C. Kang, Electrochemical properties of LiNi<sub>0.8</sub>Co<sub>0.2-x</sub>Al<sub>x</sub>O<sub>2</sub> (0 ≤ x ≤ 0.1) cathode particles prepared by spray pyrolysis from the spray solutions with and without organic additives, *Metals and Materials International* 16 (2) (2010) 299–303.
- [10] D.H. Kim, Y.U. Jeong, Crystal structures and electrochemical properties of LiNi<sub>1-x</sub>Mg<sub>x</sub>O<sub>2</sub> (0 ≤ x ≤ 0.1) for cathode materials of secondary lithium batteries, *Korean Journal of Metals and Materials* 48 (3) (2010) 262–267.
- [11] S.N. Kwon, J.H. Song, D.R. Mumm, Effects of cathode fabrication conditions and cycling on the electrochemical performance of LiNiO<sub>2</sub> synthesized by combustion and calcination, *Ceramics International* 37 (5) (2011) 1543–1548.
- [12] M.Y. Song, C.K. Park, H.R. Park, D.R. Mumm, Variations in the electrochemical properties of metallic elements-substituted LiNiO<sub>2</sub> cathodes with preparation and cathode fabrication conditions, *Electronic Materials Letters* 8 (1) (2012) 37–42.
- [13] M.Y. Song, D.R. Mumm, C.K. Park, H.R. Park, Cycling performances of LiNi<sub>1-y</sub>M<sub>y</sub>O<sub>2</sub> (M = Ni, Ga, Al and/or Ti) synthesized by wet milling and solid-state method, *Metals and Materials International* (2012), <http://dx.doi.org/10.1007/s12540-012-3013-3>.
- [14] J.M. Tarascon, E. Wang, F.K. Shokoohi, W.R. Mckinnon, S. Colson, The spinel phase of LiMn<sub>2</sub>O<sub>4</sub> as a cathode in secondary lithium cells, *Journal of the Electrochemical Society* 138 (1991) 2859–2864.
- [15] A.R. Armstrong, P.G. Bruce, Synthesis of layered LiMnO<sub>2</sub> as an electrode for rechargeable lithium batteries, *Letters to Nature* 381 (1996) 499–500.
- [16] M.Y. Song, D.S. Ahn, On the capacity deterioration of spinel phase LiMn<sub>2</sub>O<sub>4</sub> with cycling around 4 V, *Solid State Ionics* 112 (1998) 21–24.
- [17] M.Y. Song, D.S. Ahn, H.R. Park, Capacity fading of spinel phase LiMn<sub>2</sub>O<sub>4</sub> with cycling, *Journal of Power Sources* 83 (1999) 57–60.
- [18] D.S. Ahn, M.Y. Song, Variations of the electrochemical properties of LiMn<sub>2</sub>O<sub>4</sub> with synthesis conditions, *Journal of the Electrochemical Society* 147 (3) (2000) 874–879.
- [19] H.J. Guo, Q.H. Li, X.H. Li, Z.X. Wang, W.J. Peng, Novel synthesis of LiMn<sub>2</sub>O<sub>4</sub> with large tap density by oxidation of manganese powder, *Energy Conversion and Management* 52 (4) (2011) 2009–2014.
- [20] C. Wan, M. Cheng, D. Wu, Synthesis of spherical spinel LiMn<sub>2</sub>O<sub>4</sub> with commercial manganese carbonate, *Powder Technology* 210 (1) (2011) 47–51.
- [21] J.W. Park, J.H. Yu, K.W. Kim, H.S. Ryu, J.H. Ahn, C.S. Jin, K.H. Shin, Y.C. Kim, H.J. Ahn, Surface morphology changes of lithium/sulfur battery using multi-walled carbon nanotube added sulfur electrode during cyclings, *Korean Journal of Metals and Materials* 49 (2) (2011) 174–179.
- [22] Y. Nishida, K. Nakane, T. Satoh, Synthesis and properties of gallium-doped LiNiO<sub>2</sub> as the cathode material for lithium secondary batteries, *Journal of Power Sources* 68 (1997) 561–564.
- [23] P. Barboux, J.M. Tarascon, F.K. Shokoohi, The use of acetates as precursors for the low-temperature synthesis of LiMn<sub>2</sub>O<sub>4</sub> and LiCoO<sub>2</sub> intercalation compounds, *Journal of Solid State Chemistry* 94 (1991) 185–196.
- [24] J. Morales, C. Perez-Vicente, J.L. Tirado, Cation distribution and chemical deintercalation of Li<sub>1-x</sub>Ni<sub>1+x</sub>O<sub>2</sub>, *Materials Research Bulletin* 25 (1990) 623–630.
- [25] A. Rougier, I. Saadoun, P. Gravereau, P. Willmann, C. Delmas, Effect of cobalt substitution on cationic distribution in LiNi<sub>1-y</sub>Co<sub>y</sub>O<sub>2</sub> electrode materials, *Solid State Ionics* 90 (1996) 83–90.
- [26] B.J. Neudecker, R.A. Zuh, B.S. Kwak, J.B. Bates, J.D. Robertson, Lithium manganese nickel oxides Li<sub>x</sub>(Mn<sub>y</sub>Ni<sub>1-y</sub>)<sub>2-x</sub>O<sub>2</sub>, *Journal of the Electrochemical Society* 145 (1998) 4148–4157.
- [27] C. Delmas, I. Saadoun, Electrochemical and physical properties of the Li<sub>x</sub>Ni<sub>1-y</sub>Co<sub>y</sub>O<sub>2</sub> phases, *Solid State Ionics* 53–56 (1992) 370–375.
- [28] E. Zhecheva, R. Stoyanova, Stabilization of the layered crystal structure of LiNiO<sub>2</sub> by Co-substitution, *Solid State Ionics* 66 (1993) 143–149.
- [29] C. Delmas, I. Saadoun, A. Rougier, The cycling properties of the Li<sub>x</sub>Ni<sub>1-y</sub>Co<sub>y</sub>O<sub>2</sub> electrode, *Journal of Power Sources* 43–44 (1993) 595–602.
- [30] A. Ueda, T. Ohzuku, Solid-state redox reactions of LiNi<sub>1/2</sub>Co<sub>1/2</sub>O<sub>2</sub> (*R*3m) for 4 V secondary lithium cells, *Journal of the Electrochemical Society* 141 (1994) 2010–2014.
- [31] R. Alcántara, J. Morales, J.L. Tirado, R. Stoyanova, E. Zhecheva, Structure and electrochemical properties of Li<sub>1-x</sub>(Ni<sub>y</sub>Co<sub>1-y</sub>)<sub>1+x</sub>O<sub>2</sub>. Effect of chemical delithiation at 0 °C, *Journal of the Electrochemical Society* 142 (1995) 3997–4005.
- [32] Y.M. Choi, S.I. Pyun, S.I. Moon, Effects of cation mixing on the electrochemical lithium intercalation reaction into porous Li<sub>1-δ</sub>Ni<sub>1-y</sub>Co<sub>y</sub>O<sub>2</sub> electrodes, *Solid State Ionics* 89 (1996) 43–52.
- [33] K. Amine, H. Yasuda, Y. Fujita, New process for low temperature preparation of LiNi<sub>1-x</sub>Co<sub>x</sub>O<sub>2</sub> cathode material for lithium cells, *Annales de Chimie Science des Matériaux* 23 (1998) 37–42.
- [34] C.C. Chang, N. Scarr, P.N. Kumta, Synthesis and electrochemical characterization of LiMO<sub>2</sub> (M = Ni, Ni<sub>0.75</sub>Co<sub>0.25</sub>) for rechargeable lithium ion batteries, *Solid State Ionics* 112 (1998) 329–344.
- [35] S.G. Kang, K.S. Ryu, S.H. Chang, S.C. Park, The novel synthetic route to LiCo<sub>y</sub>Ni<sub>1-y</sub>O<sub>2</sub> as a cathode material in lithium secondary batteries, *Bulletin of the Korean Chemical Society* 22 (12) (2001) 1328–1332.
- [36] W. Li, J.N. Reimers, J.R. Dahn, In situ X-ray diffraction and electrochemical studies of Li<sub>1-x</sub>NiO<sub>2</sub>, *Solid State Ionics* 67 (1993) 123–130.
- [37] H. Arai, S. Okada, H. Ohtsuka, M. Ichimura, J. Yamaki, Characterization and cathode performance of Li<sub>1-x</sub>Ni<sub>1+x</sub>O<sub>2</sub> prepared with the excess lithium method, *Solid State Ionics* 80 (1995) 261–269.
- [38] T. Ohzuku, A. Ueda, M. Nagayama, Electrochemistry and structural chemistry of LiNiO<sub>2</sub> (*R*3m) for 4 V secondary lithium cells, *Journal of the Electrochemical Society* 140 (1993) 1862–1870.
- [39] M.Y. Song, D.S. Lee, H.R. Park, Electrochemical properties of LiNi<sub>1-y</sub>Ti<sub>y</sub>O<sub>2</sub> and LiNi<sub>0.975</sub>M<sub>0.025</sub>O<sub>2</sub> (M = Zn, Al, and Ti) synthesized by the solid-state reaction method, *Materials Research Bulletin* 47 (2012) 1021–1027.